This is a non-peer-reviewed preprint submitted to EarthArXiv.
It is under review in Geothermics.

Decision-making under uncertainty for shallow geothermal systems in complex subsurface settings: application to a low-transmissivity aquifer

Luka Tas[1] (https://orcid.org/0000-0001-7007-9082), Jef Caers[2] (https://orcid.org/0000-0003-0262-9905), Thomas Hermans[1] (https://orcid.org/0000-0001-9522-1540)

[1]Laboratory for Applied Geology and Hydrogeology, Department of Geology, Ghent University, Ghent, Belgium

[2]Department of Earth & Planetary Sciences, Stanford University, 450 Serra Mall, Stanford, CA 94305, USA

Correspondence: Luka Tas <luka.tas@ugent.be>

Abstract

Excess thermal energy can be stored in the subsurface and recovered when needed to heat and cool buildings sustainably. Aquifer thermal energy storage systems (ATES) are gaining popularity worldwide. Most operational systems are located in thick productive aquifers. Their efficiency and wide applicability have been proven and there is now a tendency to explore more complex settings. Aquifers with high natural groundwater flow, fractured rocks, and low-transmissivity aquifers could be added to the list of potential ATES targets. Currently, uncertainty about the systems' efficiency due to geological complexity hinders the investment in these settings. Reducing investment risk through improved decision-making becomes crucial. This paper introduces a methodology to establish a decision tree for ATES, enabling decision-makers to develop ATES systems effectively, and applies this methodology to a low-transmissivity aquifer. Decisions need to be made on two prediction targets: hydraulic feasibility and thermal feasibility. A sensitivity analysis of the output of groundwater flow and heat transport models improves our understanding of the impact of model parameters and engineering actions on both prediction targets. From that analysis, we find that storage conditions with transmissivity below 20 m^2/d lead to inefficient systems. Desirable storage conditions have transmissivity above 40 m^2/d. Thermal breakthrough risk is higher when longitudinal dispersion is above 3 m. Our approach results in some minimum system requirements in terms of subsurface properties that have to be reached for which an investment is justified. Finally, the decision tree proposes target engineering actions to decrease the investment risk while optimizing the return.

Keywords

Aquifer thermal energy storage (ATES), Hydrogeology, Decision-making, Sustainability, Optimization, Geothermal energy, Uncertainty quantification

Highlights

- New risk assessment method for ATES projects in complex subsurface settings
- Evaluate project feasibility before investing in field tests
- Include uncertainty in models and method for uncertainty quantification
- Set thresholds on critical subsurface properties to guide investment decisions
- To illustrate, the ATES decision tree is applied to a low-transmissivity aquifer

1. Introduction

In Europe, heating demand of the building sector accounts for approximately 32% of the total energy consumption, excluding the rising demand for cooling (European Commission, 2016; Ramos-Escudero et al., 2021). To mitigate the detrimental effects of climate change, it becomes therefore crucial to explore green alternatives to fulfil thermal energy demand. Low-temperature thermal energy storage systems have emerged as a promising contributor to the energy mix. Essentially, these systems store excess heat and cold of buildings in the shallow subsurface (< 200 m) in order to use it when needed. Its current success can be explained by two main aspects: a wide applicability and a high energy efficiency. First, subsurface space is widely available, and the versatility of shallow geothermal systems promotes their implementation. Secondly, the ability to store and recover excess thermal energy, while remaining unaffected by daily temperature fluctuations, makes these systems more efficient than air-source heat pumps.

Aquifer thermal energy storage (ATES) systems directly use the groundwater through pairs of pumping and injection wells storing warmer and cooler volumes of groundwater (Fig. 1). On average 0.5 kg of CO_2 can be saved for every cubic meter of pumped water (Fleuchaus et al., 2018). For heating purposes, the system relies on a heat pump to further increase the water temperature. Cooling can be achieved either actively (using pumps) or passively. To further reduce the system's environmental impact, electricity required for these pumps can be supplied by photovoltaic technologies.

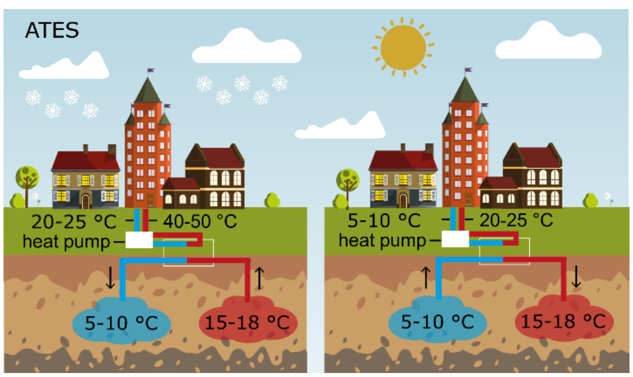

Fig. 1 Graphical representation of an ATES system in winter and summer configuration (Tas et al., 2023)

ATES systems are cost-effective in fulfilling large energy demands and are therefore suitable for hospitals, schools and large office or commercial buildings. The produced thermal energy is directly proportional to the total flow rate of the system and the temperature difference at which the water is stored compared to the natural groundwater temperature (Glassley, 2015). The higher the maximum injection and extraction flow rate, the fewer well pairs are needed to fulfil energy demand. Traditionally, thick sandy productive layers with flow rates of 100's m^3/h (in a single well pair) are the primary target for ATES (Sommer et al., 2015; Bloemendal and Hartog, 2018; Fleuchaus et al., 2018). A flow rate lower than 10 m^3/h or a transmissivity lower than 50 m^2/d is commonly considered not feasible and economically less interesting (François and Van Lysebetten, 2017). This traditional view on the potential areas for aquifer thermal energy storage is evolving, influenced by an increasing interest in these systems. It is driven by the uncertain energy cost, governmental incentives for green energy investments and increasing competition with other groundwater uses in the most productive aquifers (Bloemendal et al., 2018; Stemmle et al., 2024). This translates into investments in aquifers that are more complex and at the limit of suitability for ATES.

Current challenges for further application of ATES systems are mostly related to the high initial investment cost, linked to the drilling and completion of the wells, and uncertainties about the prediction of the energy efficiency (Winter, 2004; Hermans et al., 2019; Heldt et al., 2024). Because of limited in-situ measurements, we cannot perfectly characterize the hydraulic and thermal transport parameters in the subsurface. This means we cannot be 100 % certain that a model accurately represents reality, even when it is able to confirm data from field tests (White et al., 2014). In cases where the target aquifer is predominantly homogeneous, uncertainty remains limited and does not jeopardize ATES implementation (Doughty et al., 1982; Bloemendal and Hartog, 2018). For more complex ATES targets, the story is different. There, uncertainties on subsurface properties might have a significant effect. For instance, a high natural gradient in a gravel layer of an alluvial aquifer can result in an extremely low efficiency due to a total loss of stored thermal energy (De Schepper et al., 2020; Silvestri et al., 2025; Tas et al., 2025). Similarly, in chalk or fractured rock formations, preferential flow paths are present which can quickly transport the stored thermal energy away or create a short circuit between the warm and cold wells causing a failure of the system (Sommer et al., 2013; De Paoli et al., 2023; Regnier et al., 2023; Jackson et al., 2024). Also in low-transmissivity aquifers there is considerable uncertainty about the return on investment. These aquifers are characterized by low productivity, which has two main consequences. First, the investment cost to meet energy demand significantly rises due to the need for more drillings. Second, subsurface uncertainties become more critical because the system must operate close to the maximum aquifer capacity. Excessive pressure changes in the wells should be avoided to mitigate the risk of well collapse or surface flooding. Additionally, when operating many wells simultaneously, the design (extraction) flow rate must still be achievable and a thermal short circuit between wells must be avoided. Consequently, low-transmissivity aquifers currently remain an untapped resource. Nevertheless, ATES systems can still lead to up to 50% cost savings compared to the closed-loop borehole thermal energy storage (BTES) alternative (generally used to fulfill small energy demands of a single household) (Tas et al., 2023).

Currently, the only common method to mitigate subsurface uncertainties and, consequently, the uncertainty about return on investment, is to do more field tests. However, this approach inherently further raises the initial investment cost and overlooks the potential inaccuracy and limited spatial representativeness of field data. Therefore, this approach still fails to acknowledge uncertainty about the predicted energy efficiency and it does not support communication of investment risks to decision-makers. To sustain market growth for ATES systems and encourage their broader applicability in complex subsurface settings, this paper develops a method to improve feasibility studies and applies it to a low-transmissivity setting. We aim to draw a step-by-step decision tree which supports the go/no go decision of the investment. To do so, a stochastic approach is used because it allows to consider a range of possibilities instead of providing a single truth/prediction (Renard, 2007; Ferré, 2017). This offers valuable insights into which parameter combinations lead to the most or least economically viable conditions for a given hydrogeological setting before investing in field tests. Additionally, it enables risk and uncertainty analysis, as well as quantification of the impact of mitigating measures to reduce the risk. This is crucial for informed decision-making in ATES projects, particularly those operating near the limits of natural boundaries. To our knowledge, such an approach has not yet been explored in the context of shallow geothermal energy.

2. Overview

We aim to establish a decision tree that can support decision-makers in making informed investments in ATES systems. This approach aims to provide an easy-to-interpret and clear overview of the aspects that should be considered during a feasibility study. It should visualize the connections between prediction targets, most informative subsurface properties, intermediate decisions or actions that can reduce the investment risk, and the final decision.

The prediction targets serve as the main nodes of the decision tree. If multiple targets are relevant to determine feasibility, their importance should be ranked. The root node of the decision tree should correspond to the critical prediction target. From the root node, different branches grow that represent categories of relevant subsurface properties. Based on these categories, a first feasibility assessment can be done. If this preliminary assessment is insufficient to guarantee feasibility, a secondary assessment can be made using a more thorough uncertainty quantification and risk assessment. For such edge cases, the decision tree can include proposals for engineering actions to enhance feasibility. Once the critical prediction target has been positively assessed, the decision tree should proceed to the next prediction target, which acts as a secondary root node. The outermost branches of the decision tree represent the final decision. The action to model the full ATES system in detail should only be proposed just before the final decision is made. This approach ensures that the most time- and cost-intensive step of a feasibility study is only undertaken when there is sufficient certainty about the project's feasibility. If the investor or government has specific requirements regarding the prediction targets, these can be included right below the root nodes, ensuring they are evaluated and considered from the start.

Figure 2 shows the suggested workflow to arrive at such a decision tree. First, a benchmark model and the prediction targets (root nodes) should be defined based on the hydrogeological setting we aim to evaluate. Second, a decision-focused uncertainty quantification involves stating prior model variables and their distribution. This is part of the Monte Carlo study and depends on the uncertain variables and engineering actions we aim to evaluate. Monte Carlo simulations allow bringing prior uncertainty into the analysis. It generates an output that can be used for analysis of probability distributions and makes the results applicable beyond the benchmark model. Third, the model output is processed with a global sensitivity analysis (here distance-based global sensitivity analysis (DGSA)) to understand the effect of parameters and key decision variables. On the one hand, SA can improve our understanding by identifying the sensitive parameters and by analyzing the parameter space leading to desirable storage conditions or conditions to be avoided. We aim to define criteria on sensitive subsurface parameters for the decision tree (categories of subsurface properties in the decision tree). On the other hand, SA results can serve as a basis for uncertainty quantification. Specifically, we statistically analyze the relation between sensitive parameters and prediction targets. This aims to make better-informed decisions for edge cases (actions in the decision tree). This workflow can be followed prior to the availability of field data. Below, the details of this workflow are discussed and applied to a low-transmissivity setting.

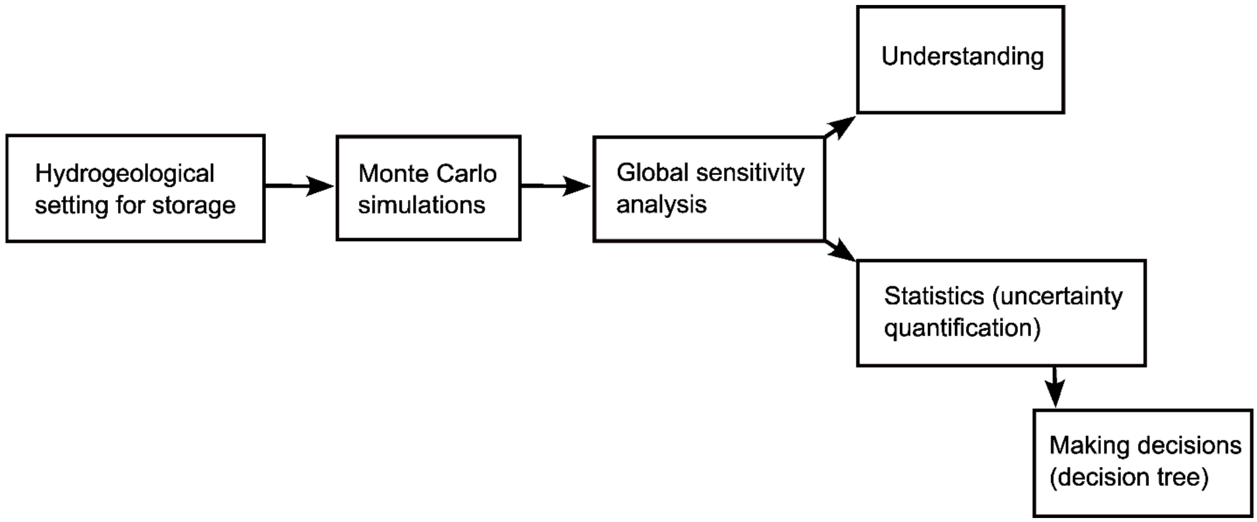

Fig. 2 Suggested workflow to improve understanding and decision-making for ATES systems using a stochastic approach

3. Methodology

3.1. Hydrogeological setting for storage

3.1.1. Layered low-transmissivity aquifer

The proposed workflow to arrive at a decision tree is applicable to any hydrogeological setting for storage. To illustrate the benefits of the proposed workflow in the field of shallow thermal energy storage, it is applied to a layered low-transmissivity aquifer. In this kind of aquifer, the ATES system will consist of several well pairs functioning at maximum aquifer capacity, presenting the following main challenges (Tas et al., 2023):

1. What are the limits on injection/extraction rates to avoid excessive pressure changes in wells?
2. How close can the wells be placed to each other without inducing a thermal short circuit?

Therefore, the decision tree for low-transmissivity settings should evaluate two main prediction targets:

1. hydraulic feasibility, assessed as the head change in the wells over time ($\Delta H(t)$)
2. thermal feasibility, assessed as the temperature evolution in the wells over time ($\Delta T(t)$).

From a practical point of view, hydraulic feasibility is critical (primary root node). As such, depending on the maximum allowable head change in the aquifer, the decision tree should distinguish between different categories of subsurface properties that lead to feasible/excessive head changes. Thermal feasibility or high energy efficiency is desirable (secondary root node). Currently, no minimum target efficiency is required by law, but the investor might favor highly efficient systems. The main concern is therefore avoiding thermal breakthrough conditions leading to very low system efficiency.

3.1.2. Benchmark model and data description

In the benchmark model for the stochastic analysis, the aquifer system for storage is very shallow and ranges from 10 to 50 m deep (Fig. 3). Three semi-permeable layers, composed of sandy clays, are alternated by three more permeable layers, composed of clayey sands. The total transmissivity of the permeable part was estimated to be about 20 m^2/d (Lebbe et al., 1992). The maximum estimated flow rate of 5 m^3/h is significantly below the standard cutoff rate of 10 m^3/h. This conceptual model of a low-transmissivity aquifer is based on the hydrogeology at the Ghent University Faculty of Science campus (Belgium). Descriptions of lithology, borehole geophysical data and hydraulic head measurements are used to create a realistic base-case model (Lebbe et al., 1992). The Monte Carlo simulations include broad variability around this benchmark, making the results of this study applicable across a diverse range of low-transmissivity settings (see 3.2).

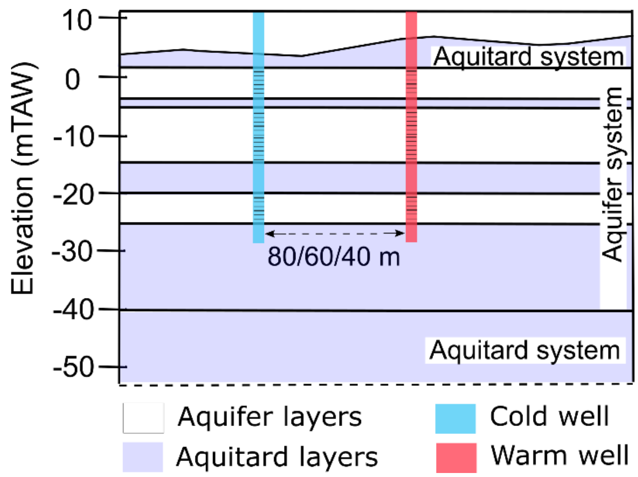

Fig. 3 Graphical representation of the study case. The layered aquifer system consists of 3 aquifer layers and 3 aquitard layers. One warm and one cold well are considered, screened in the permeable layers of the aquifer system

For simplicity, the groundwater flow and heat transport model simulates a single well pair consisting of one warm and one cold well (Fig. 3). The base model covers an area of 1 by 1 km centered around the cold and warm wells which are placed perpendicular to natural groundwater flow. The hydraulic gradient is imposed from north to south and is centered around the initial head of 6.75 m. Each well is screened in all three aquifer layers. Maximum horizontal cell size of the structured grid is 20 m and gradually refines to 1 m in an area of 40 by 40 meters around each well. The top of the model is 10.4 mTAW (meters above average sea level at low tide). The model bottom corresponds to the lower limit of the Aquifer system at -40.6 mTAW. Below, a 95 m thick clay layer is present (Databank Ondergrond Vlaanderen, n.d.). The low-transmissivity aquifer is subdivided into thinner layers of approximately 1 m thickness to accurately represent heat transfer processes between aquifers and aquitards. Only the upper part of the model top is more coarsely subdivided (maximum 8 m) because it is modeled as unconfined. It was confirmed that the solution does not become more accurate with further reduction in grid cell size (White et al., 2020). The original hydraulic and thermal subsurface parameters of the base model can be consulted in Table 1.

The flow boundary conditions include:

1) A constant head boundary for the north, south, east and west boundaries to represent the natural hydraulic gradient.
2) A recharge boundary for the model top to impose recharge from rainfall (190 mm/y).
3) Multi-node wells with a diameter of 125 mm to distribute the pumping and injection rate across the aquifer layers and to account for well losses (based on the Thiem equation) (Konikow et al., 2009).
4) No-flow boundary for the bottom of the model.

For heat transport, all model boundaries are set to the natural average aquifer temperature of 13.8 °C, except for the bottom boundary which is zero-dispersion/diffusion heat flux. Water is generally injected with a temperature difference of 5 °C compared to the natural aquifer temperature. For ΔT(t) it is important to note that the data is saved with a daily time discretization and is averaged over all aquifer sub-layers. In this study, the thermal recovery efficiency of the ATES system is defined as the percentage of thermal energy that can be extracted from the energy that was stored during the previous season (Duijff et al., 2021).

The modelled scenario represents the cyclic operation of an ATES system starting with a summer season. Water is extracted from the cold well and heat is stored for 6 months at a constant flow rate and temperature difference. The system is reversed during the following winter season, implying a yearly balance between heating and cooling demand. This scenario is repeated three times in total, representing the first 3 years of operation. In the model, each season is represented by one stress period subdivided into 60 time steps according to a multiplier of 1.2.

The freely available USGS MODFLOW 2005 software (v1.12.00) is used to simulate groundwater flow (Harbaugh et al., 2017). The preconditioned conjugate gradient (PCG) package is used to solve the groundwater flow equation. Default settings are retained, except for HCLOSE and RCLOSE, which are decreased to 1E-5 to reach convergence.

To model heat transport processes, MT3D-USGS is used (Bedekar et al., 2016), taking advantage of the analogy between the heat and solute transport equations (Hecht-Méndez et al., 2010; Sommer et al., 2013). Water density is considered constant which is a fair assumption for a low-temperature ATES system (ΔT< 15°C) (Zuurbier et al., 2013; Zeghici et al., 2015). An implicit finite-difference method was used that applies the generalized conjugate gradient (GCG) solver for dispersion, sink/source and reaction terms. The convergence criterion of relative concentration was set to 10^{-10} as recommended by Vandenbohede et al. (2014). The total variation diminishing method (TVD) was proven suitable to solve the advection-dispersion transport equation. The Courant number (PERCEL), which determines the initial step size was set to 0.5. The Python package Flopy is used to efficiently run all simulations for the stochastic analysis (Bakker et al., 2016; Hughes et al., 2024).

3.2. Monte Carlo study

A broad uncertainty range, within reasonable limits for a low-transmissivity aquifer, was defined for the stochastic analysis. Uncertainty is included on subsurface parameters and variability on engineering actions is considered. This means that the model can represent various similar low-transmissivity settings. All parameter prior distributions are modelled with uniform distributions. From this prior distribution, random variations on the base model are generated. A Latin Hypercube sampling method ensures good coverage of the multi-dimensional parameter space (Heldt et al., 2024).

3.2.1. Subsurface uncertainties

For the aquifer system, the subsurface uncertainties include hydrogeological parameters, thermal parameters as well as boundary conditions (Table 1). Uncertainty can stem from limited data density, questionable accuracy of field tests or absence of proper estimates from literature (Winter, 2004; Renard, 2007; Xu and Valocchi, 2015; Beernink et al., 2022). The natural hydraulic gradient, thickness, and hydraulic conductivity govern the groundwater flow processes in the aquifer. The longitudinal dispersivity, together with advective transport impacted by the effective porosity, contributes to heat transport through dispersion processes. The total porosity plays an important role in heat transport by conduction through the molecular diffusion coefficient (Zheng, 2010; Bloemendal and Hartog, 2018; Tas et al., 2025).

Table 1 Ranges of subsurface uncertainties of the aquifer system and variability on engineering actions that are included in the prior. The original values are validated based on (Lebbe et al., 1992; Vandenbohede et al., 2011; Tas et al., 2023)

Parameter	Unit	Original value		Range of variation	
Hydrogeological parameters low-transmissivity aquifer					
		aquifer (aqf)	aquitard (aqt)	aquifer (aqf)	aquitard (aqt)
Horizontal hydraulic conductivity (K_h) *	m/s	9.9E-6 – 1.5E-5	2.3E-8 – 4.6 E-7	U[5E-06 – 5E-05]	U[1E-08 – 1E-06]
Vertical hydraulic conductivity (K_v) *	m/s	1.1E-8 – 1.1 E-5	8.6E-9 – 3.1E-7	U[5E-07 – 2.5E-05]	U[1E-09 – 5E-07]
Total porosity (n_t/*Tot. por.*) *	-	0.35		U[0.20 – 0.50]	U[0.40 – 0.70]
Effective porosity (n_e/*Eff. por.*) ~ specific yield (S_y) *	-	0.3		U[0.10 – 0.40]	U[0.02 – 0.14]
Specific storage (S_s)	m^{-1}	1.2E-5 – 5.5E-5		–	
Total thickness aquifer layers (*Thick.*) *	m	18.5		U[14.7 – 22.3]	
Longitudinal dispersion (α_l/*Long. disp.*) *	m	–		U[1 – 5]	
Density water (ρ_w)	kg/m^3	1000		–	
Density solid (ρ_s)	kg/m^3	2640		–	
Bulk density (ρ_b)	kg/m^3	$\rho_s \times (1 - n_t)$		[1320 – 2112]	[792 – 1584]
Thermal conductivity water (k_w)	W/(m°C)	0.58		–	
Thermal conductivity solid (k_s)	(W/(m°C)	3	2	–	
Bulk thermal conductivity (k_b)	(W/(m°C)	$k_w \times n_t + k_s \times (1 - n_t)$		[1.79 – 2.52]	[1.0 – 1.43]
Specific heat capacity solid (c_s)	J/(kg°C)	730	1381	–	
Specific heat capacity water (c_w)	J/(kg°C)	4183		–	
Thermal distribution coefficient (K_d)	m^3/kg	$c_s/(c_w \times \rho_w)$		–	
Effective molecular diffusion coefficient (D_m)	m^2/s	$k_b \div (\mathrm{n}_t \times \rho_w \times \mathrm{c}_w)$		[8.6E-7 – 3.0 E-6]	[3.4E-7 – 8.6E-7]
Boundary conditions					
Natural groundwater temperature (T_0)	°C	13.8		–	
Natural hydraulic gradient (*Grad.*) *	%	0.13		U[0 – 0.3]	
Engineering actions					
Flow rate *	m^3/h	5		U[3-6]	
Well spacing *	m	80		80, 60, 40	
Injection ΔT	°C	5		–	

* For these parameters, a random value within the range of variation was selected for the analysis

The vertical hydraulic conductivity is a variable ratio from the horizontal hydraulic conductivity, and the effective porosity is calculated as a percentage of the total porosity. Aquifer and aquitard layers have variable thicknesses but the total thickness of the low-transmissivity aquifer remains constant (when the aquifer thickness increases, the aquitard thickness decreases). The relative thickness of each layer compared to the total aquifer/aquitard thickness also remains constant.

3.2.2. Variability on engineering actions and decision problem

Next to uncertainties that are inherent to the subsurface, there are also diverse engineering actions that influence the system's efficiency (Bloemendal et al., 2018). Flexibility in these actions allows optimizing ATES systems in shallow aquifers or at least reduce the economic and technological risks.

As mentioned earlier, the thermal energy is directly proportional to the total flow rate and the temperature difference between the injected water and the natural groundwater. Often, a temperature difference of 5 °C is considered to be standard. However, operating the ATES system at 6 or 7 °C temperature difference allows reducing proportionally the flow rate per well pair or the number of wells. This is a useful variable when operating a system at the aquifer limits. Depending on whether the priority is decreasing the pressure in the wells, fitting the wells in the available space, or reducing the initial investment cost related to the drilling, one of these two options will be preferred to alleviate the uncertainty/risk related to the decision. Uncertainty on ΔT of injection (U[5-7] °C) is not included in the sensitivity analysis because it is logically, and by far, the most sensitive parameter for ΔT(t), while it does not impact ΔH(t). However, it is still considered as variable in the decision problem.

The maximum flow rate is randomly sampled within U[3-6 m^3/h] (Table 1). This allows us to consider opportunities that aim to increase hydraulic feasibility. Lower flow rates represent systems with more well pairs or systems designed not to cover the rarely reached peak demand. While engineering actions are not random variables, to generate such variable actions, we sample them from uniform distributions with ranges specified by the limits of the system.

Finally, the distance between the warm and cold storage wells can be adjusted. On the one hand, this needs to be large enough to avoid thermal breakthroughs. On the other hand, it was shown that a smaller well spacing between warm and cold wells would be beneficial to counterbalance high injection pressures in low-transmissivity settings (Tas et al., 2023). Three scenarios are modelled, each with a different distance between both wells (80m,60m,40m) (Fig. 2, Table 1). For each scenario, 500 model realizations are sampled and simulated. This number is obtained by trial and error but is sufficient to get consistent SA results (e.g., Zhang et al., 2025).

3.3. Clustering and sensitivity analysis

The distance-based global sensitivity analysis (DGSA) method was used for the sensitivity analysis. Compared to the Sobol or Morris method, it stands out by its flexibility and computational efficiency while remaining statistically significant (Scheidt et al., 2018). In essence, the strong influence of sensitive parameters allows clustering the model responses. For each parameter, the DGSA method calculates the sensitivity based on the (dis)similarity between the cluster cumulative distribution functions (Fenwick et al., 2014; Park et al., 2016; Lu and Ricciuto, 2020). Clustering and DGSA is applied to both prediction targets (ΔH(t) and ΔT(t)). Using the k-means method, three clusters of the ΔH(t) prediction (representing models with large, medium and small head changes) and two clusters of the ΔT(t) prediction (representing models with a high and low thermal recovery efficiency) are distinguished. The number of clusters was optimized based on the Davies-Bouldin index and the mean silhouette index (Davies and Bouldin, 1979; Kaufman and Rousseeuw, 1990). The k-medoids clustering method was also tested and yielded similar results.

Outliers dominated by numerical dispersion and non-convergent models are excluded from the analysis. Not all random model realizations could terminate successfully with the same solver settings for the flow and transport equations. Such cases were limited to a maximum of 8 model realizations.

3.4. Uncertainty quantification

Uncertainty quantification of the maximum head change supports go/no-go investment decisions in suboptimal conditions. For the uncertainty quantification itself, we opt for a methodology that explores the entire parameter space in the low-transmissivity setting. We investigate to what extent this kind of output can be used to optimize the decision-making over a broad possibility of subsurface settings. We use kernel density estimation (KDE) because only few parameters matter in determining the head change (Silverman, 1986; Scheidt et al., 2018). Specifically, we statistically analyze the relation between sensitive parameters and prediction targets. We model the posterior uncertainty of head change given an estimate for the sensitive parameters available from field or literature data. It determines the probability of excessive head changes and allows to evaluate how engineering actions can mitigate the risk. It provides crucial and easy-to-interpret information for communication with decision-makers. When the field or literature data itself is uncertain we can take into account all possibilities and decide based on the worst-case scenario. With this approach, we aim to make general decision recommendations.

4. Results

4.1. Clustering and sensitivity analysis

4.1.1. Prediction of the change in hydraulic head ΔH(t)

For simplicity, only the results of the cold well are shown, as those of the warm well are identical but mirrored. The distance between the warm and cold wells influences head changes. The average head change in each cluster appears slightly smaller for the 40 m scenario than for the 80 m scenario (Fig. 4). This is attributed to the principle of superposition: injection and extraction counterbalance each other's influence on the head change when the inter-well distance is small (Fig 4c). Reducing the inter-well distance to 60 m is insufficient to reduce the maximum head change. It is important to note that in low-transmissivity aquifers multiple well pairs are needed and that the observed effect might be more pronounced when surrounding 1 cold well with 4 warm wells in a checkerboard pattern (Tas et al., 2023).

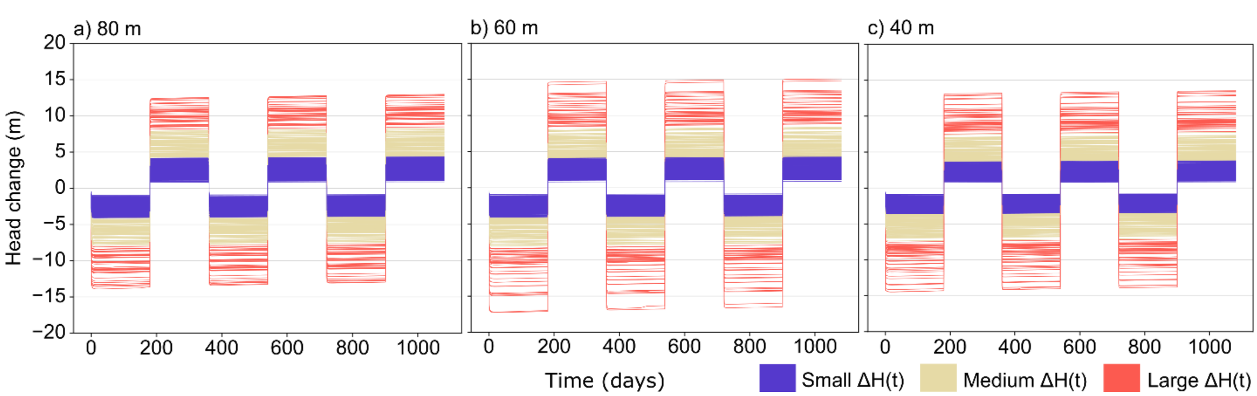

Fig. 4 Clustering of the change in head over time in the cold well for the three scenarios with decreasing distance between the warm and cold wells (a, b, c)

The DGSA results reveal an increasing number of sensitive and critical parameters with decreasing inter-well distance (Fig. 5). The main parameters dominating the ΔH(t) prediction are the vertical and horizontal hydraulic conductivity of the aquifer layers. Understandably, the flow rate significantly influences ΔH(t). For small inter-well distances, the hydraulic conductivity and thickness of the aquitard layers are also influential.

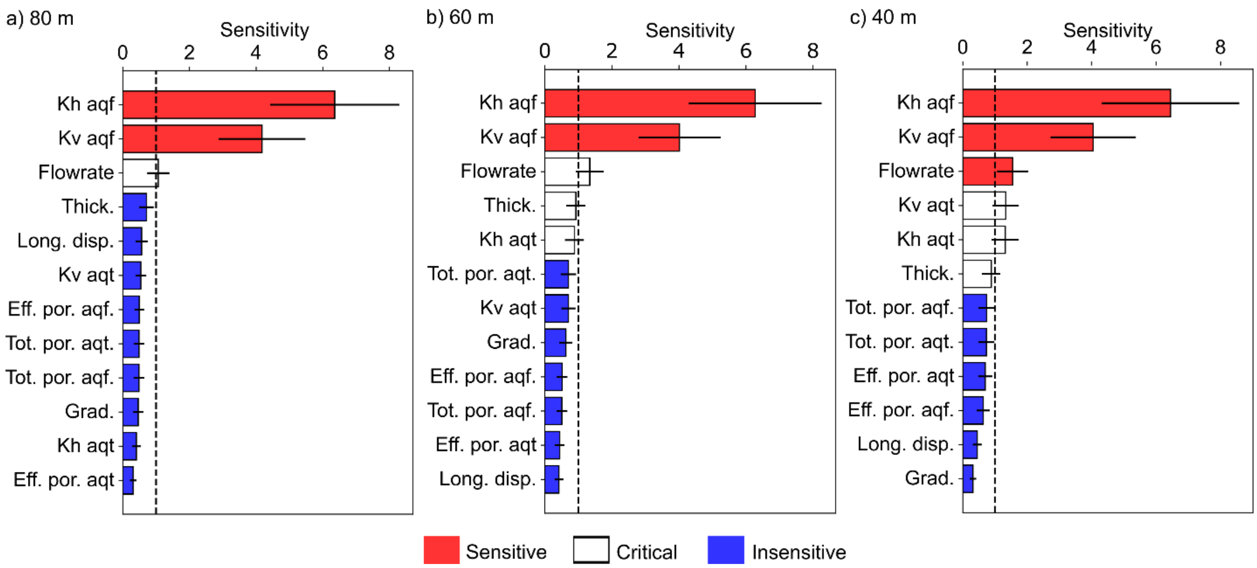

Fig. 5 Results of the DGSA of ΔH(t) with confidence interval for the three scenarios with decreasing well spacing (a, b, c)

As expected from Darcy's law, there is a sensitive interaction between aquifer horizontal hydraulic conductivity and flow rate and between aquifer horizontal hydraulic conductivity and total aquifer thickness. Together, these two parameters determine the transmissivity of the aquifer layers (Fig. 6).

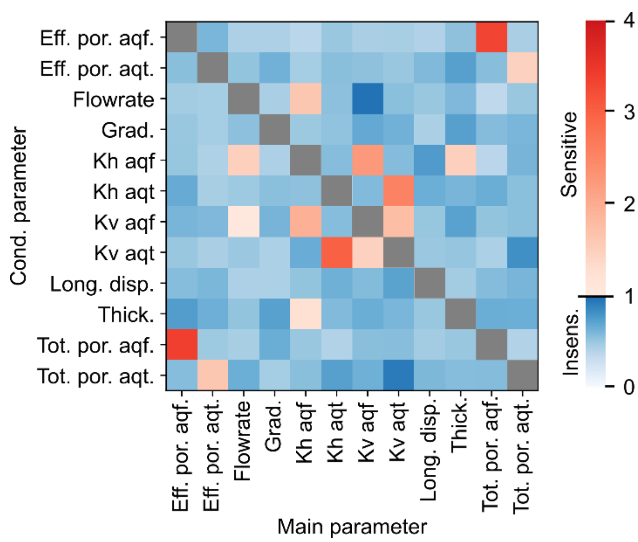

Fig. 6 Sensitivity matrix showing sensitive interactions for the scenario with 40 m well spacing

4.1.2. Prediction of the temperature difference ΔT(t)

For simplicity, ΔT(t) represents the temperature difference between the warm and cold wells (higher ΔT(t) reflects higher thermal recovery efficiency). The distance between wells affects head changes but also significantly affects thermal recovery efficiency. Figure 7 illustrates that larger inter-well distances result in higher temperature differences between warm and cold wells. In other words, thermal recovery efficiency declines as the inter-well distance decreases (Fig. 8). As hydraulic interactions between the wells increase, so will thermal interactions. Few model realizations of the 40 m scenario drop below a ΔT of 5 °C, indicating a short circuit or thermal breakthrough between both wells (Fig. 7c). Such negative thermal interactions have also been observed in traditional ATES settings due to the currently growing density of ATES systems (e.g. Duijff et al., 2021).

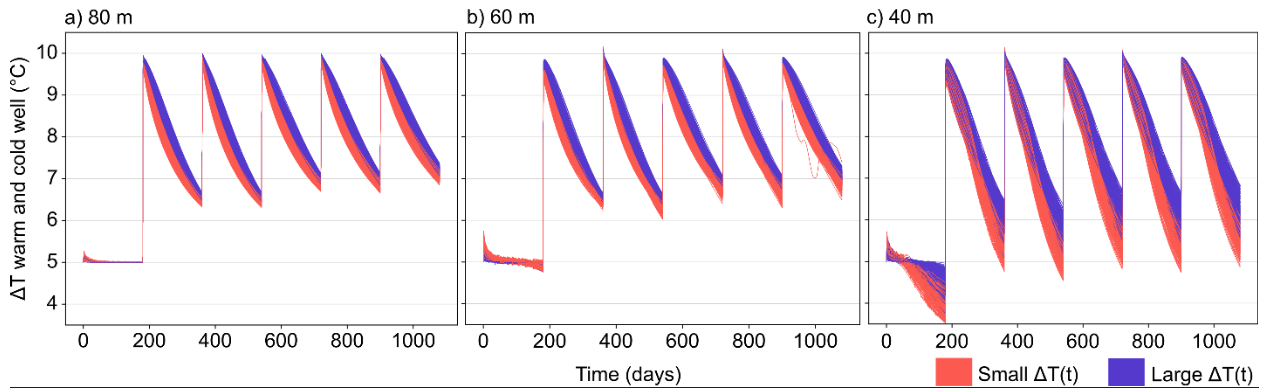

Fig. 7 Evolution of the temperature difference over time for the three scenarios (a, b, c) with decreasing distance between the warm and cold wells

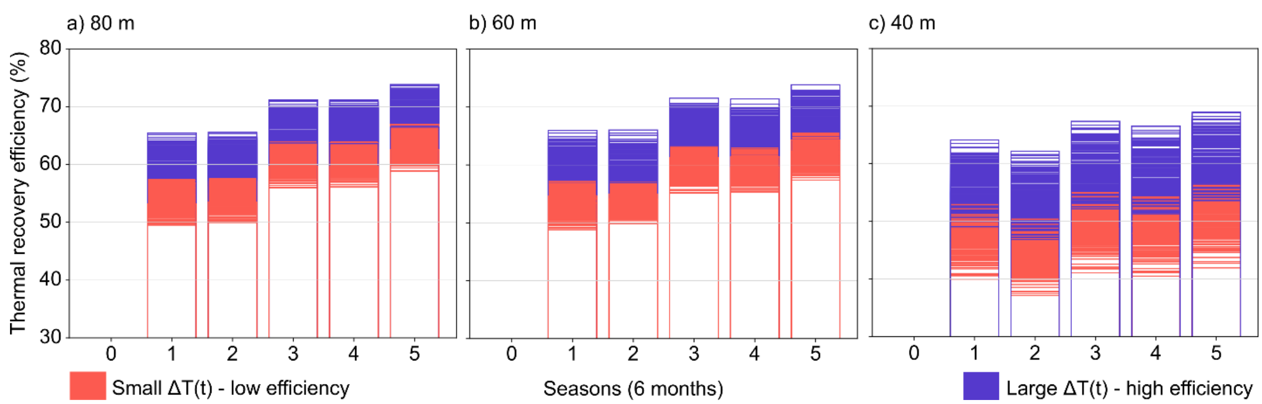

Fig. 8 Comparison of the thermal recovery efficiency for the three scenarios with different well spacing (a, b, c)

The DGSA of ΔT(t) consistently identifies longitudinal dispersion as sensitive (Fig. 9). In a low-transmissivity setting, total aquifer thickness and maximum flow rate remain limited. Therefore, the thermal radius of influence is relatively small. In this setting, the buffering effect of conduction will be smaller, explaining the influence of longitudinal dispersivity. This is opposed to traditional settings, where thermal dispersion can be neglected compared to conduction (Hopmans et al., 2002; Vandenbohede et al., 2011).

For both the 80 m and 60 m scenarios, the flow rate, thickness and total porosity of aquitard layers are sensitive or critical parameters. The flow rate, together with the aquifer thickness, determines the storage volume geometry and thus the extent of the thermal losses (Bloemendal and Hartog, 2018). The sensitivity to total aquitard porosity means that heat exchange between the aquifer and aquitard layers is an important process in layered low-transmissivity settings. Next to this, the effective and total aquifer porosity are common sensitive/critical parameters for the 80m and 40m scenarios. This highlights the influence of both conductive and dispersive heat transport processes in the aquifer layers. However, it is important to realize that the total and effective porosity are also dependent on each other in the prior.

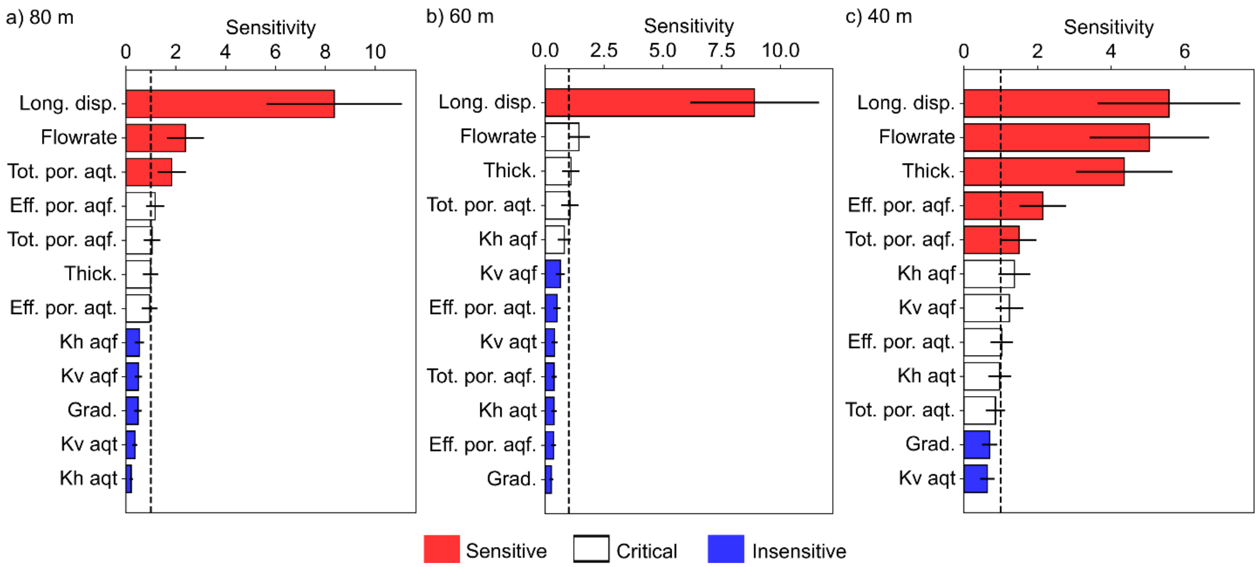

Fig. 9 Results of the DGSA of $\Delta T(t)$ with confidence interval for the three scenarios with decreasing well spacing (a, b, c)

In all three scenarios, longitudinal dispersion and flow rate exhibit a sensitive interaction (Fig. 10). Dispersion is driven by the displacement of water, caused by the flow rate of wells. In the 60 m scenario, longitudinal dispersion and hydraulic gradient show a sensitive interaction. Displacement of groundwater does not only occur due to the flow rate of wells but also due to the aquifer's natural flow. Finally, for the 40 m scenario, a sensitive interaction arises between total aquifer thickness and longitudinal dispersion. This highlights the influence of the storage volume geometry on thermal losses as also shown by Bloemendal & Hartog (2018) in the traditional ATES setting .

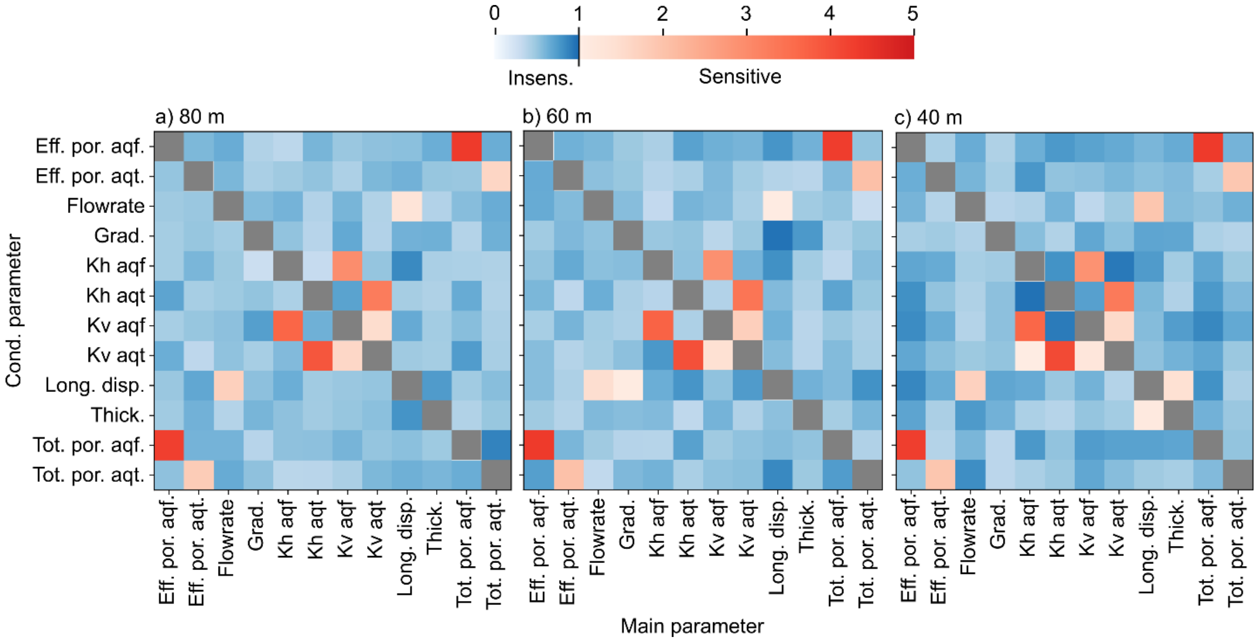

Fig. 10 Sensitivity matrix showing sensitive interactions for the three scenarios with decreasing distance between the wells (a, b, c)

4.2. Criteria on subsurface properties for decision-making

To decide about investing in ATES in low-transmissivity settings, we need scientifically sound criteria (categories) on subsurface properties for the decision tree. We propose to use the DGSA results for this (Fig. 2). Sensitive parameters are analyzed pairwise, and their probability densities are addressed. As such, the clusters reveal combinations leading to large/medium/small head changes and high/low thermal efficiency. The 40 m scenario is selected for this analysis, as it has most sensitive parameters and the highest risk for thermal breakthrough.

4.2.1. Which storage conditions should be avoided?

As a first target, excessive head changes during injection should be avoided. In this case, the maximum acceptable change has been estimated at 3.7 m based on well stability and risk of surface flooding. It corresponds to the difference between the initial piezometric level and the ground level. It exceeds the limit by NVOE (2021) standards ($max\ head\ change = 0.2 \times screen\ top\ depth$) but showed feasible in practice (Tas et al., 2023). All realizations in the red cluster (head change > 7.5 m) largely exceed this criterion, indicating that the corresponding parameter/engineering action combinations are not suited for ATES (Fig. 4).

Figure 11 shows that horizontal hydraulic conductivity is the key parameter governing head change. For this parameter there is least overlap between cluster probability density functions (pdf's). Nevertheless, the overlap indicates that other parameters such as flow rate, aquitard horizontal hydraulic conductivity and total aquifer thickness still contribute. For an aquifer horizontal conductivity below 1.15E-5 m/s, the probability density function shows that there is a higher likelihood for head changes to exceed 7.5 m. As such, conditions with an aquifer hydraulic conductivity lower than 1.15E-5 m/s are not suitable for ATES. For hydraulic conductivity above this criterion, head changes remain more limited and potentially below the practical maximum acceptable head change of 3.7 m (approximately corresponding to realizations in the purple cluster).

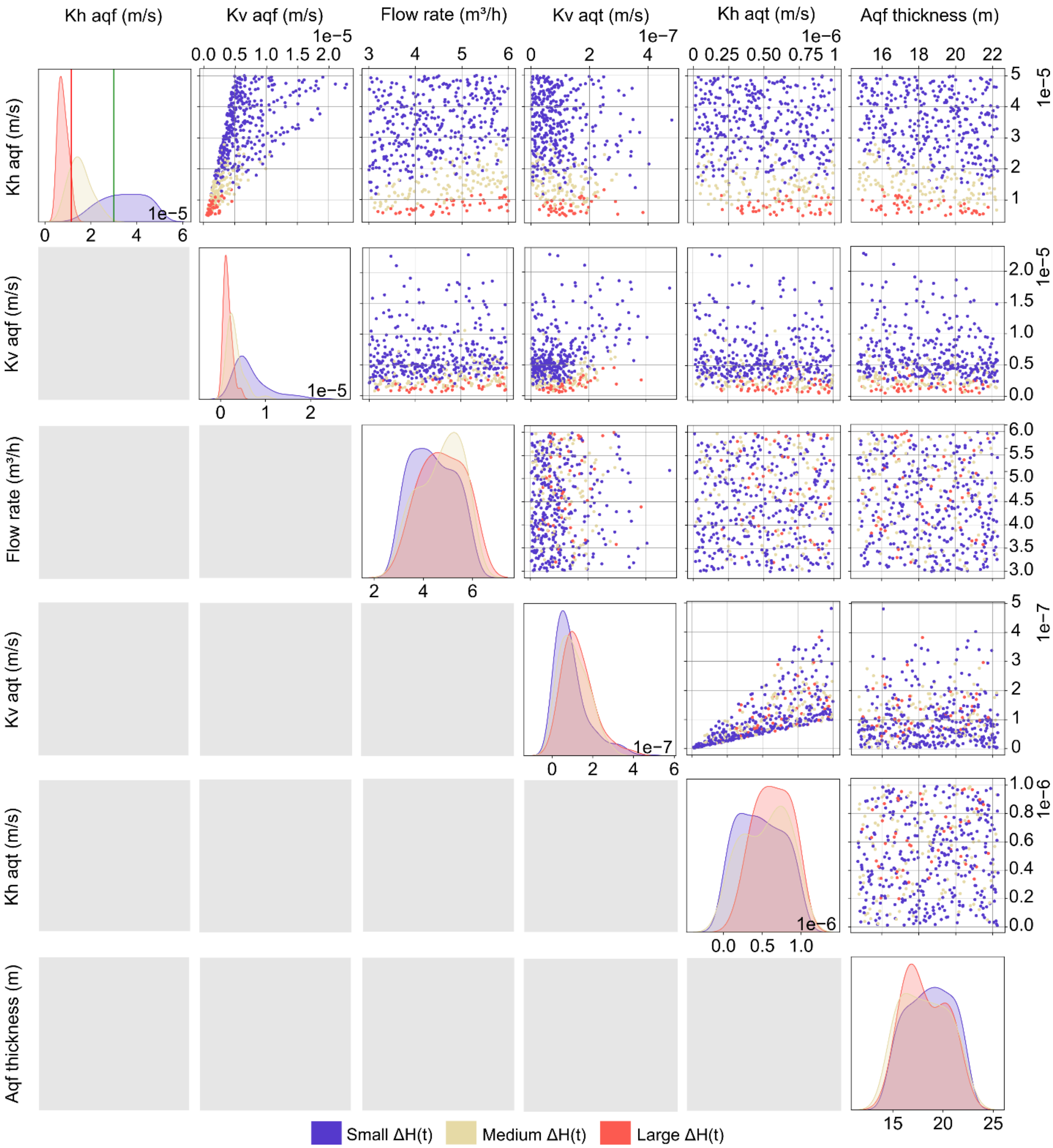

Fig. 11 Pairwise comparison of the sensitive parameters for all models. The models are colored according to the clusters of ΔH(t). The parameter probability density for each cluster is shown on the diagonal. The criteria for decision-making are indicated in red and green. The part below the diagonal is blank because the interactions are symmetric

From a thermal point of view, thermal breakthrough conditions should be avoided. The parameter distributions in Figure 12 show that a large dispersion in combination with a small total aquifer thickness and a relatively large flow rate result in the least efficient ATES systems. Longitudinal dispersion is the key sensitive parameter, also for larger inter-well distances (Fig. 9). In general, conditions with longitudinal dispersion larger than 3 m should be avoided (Fig. 12).

4.2.2. *What are the desired storage conditions?*

The decision tree should also include criteria on subsurface properties that ensure hydraulic and thermal feasibility. To guarantee limited head changes, high aquifer hydraulic conductivity is crucial. Figure 12 shows that horizontal conductivity above 3E-5 m/s results in desirable hydraulic conditions regardless of other sensitive parameters. This corresponds to the model realizations in the purple cluster without overlap with other clusters. They have a predicted maximum head change smaller than 4 m, which is feasible in practice for this low-transmissivity setting (Fig. 4).

All conditions in the 40 m scenario are suboptimal for achieving high thermal recovery efficiency. During the recovery period, the temperature drops significantly for all model realizations (Fig 7c). Only increasing inter-well distance substantially improves recovery efficiency (Fig. 8). However, as we only evaluated three inter-well distance scenarios, no criteria to guarantee high efficiency could be determined. We can only state that inter-well distance above 60 m is sufficient but it could be reduced for optimal subsurface space usage (Fig. 8). It is currently left in the investor’s interest to prioritize high energy efficiency and it is also preferred for optimal subsurface management (Heimovaara and Trcka, 2012; Stemmle et al., 2024). When targeting a minimum efficiency, uncertainty quantification can determine the likelihood of achieving it.

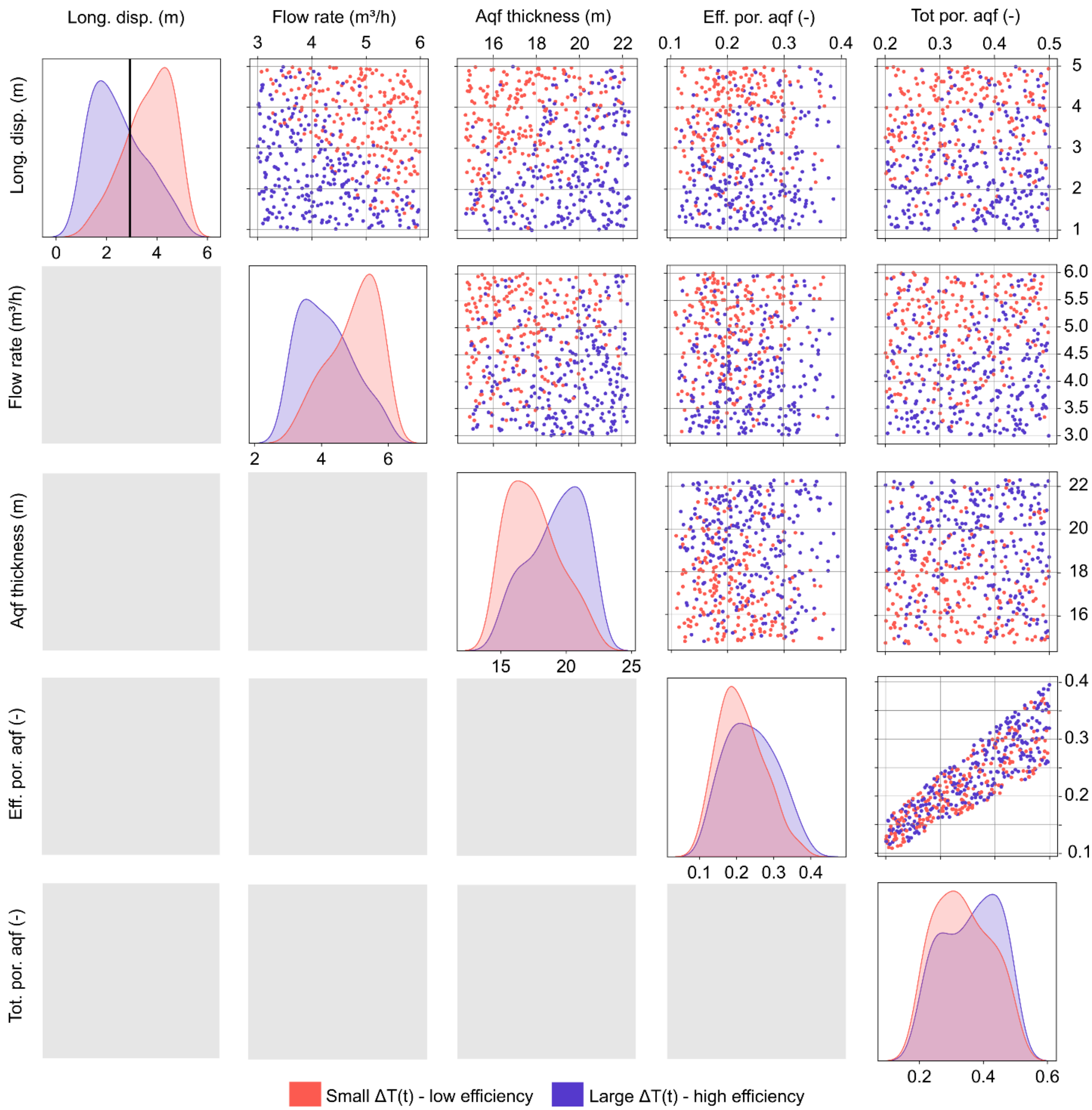

Fig. 12 Pairwise comparison of the sensitive parameters for all models. The models are colored according to the clusters of ΔT(t). The parameter probability density for each cluster is shown on the diagonal. The part below the diagonal is blank because the interactions are symmetric

4.3. Uncertainty quantification of the maximum head change

Investment decisions should not rely solely on avoiding undesirable hydraulic conditions or identifying optimal conditions. Determining whether investments in suboptimal conditions are worthwhile requires quantifying uncertainty. This is an action that is proposed in the decision tree to explore the feasibility of the target in more detail. The applicability limit of ATES in suboptimal conditions is determined by evaluating the likelihood of exceeding the maximum allowable head change, constrained by field or literature data. A risk-neutral (P50) or risk-averse (P90) decision maker can be considered. When the probability of excessive head changes is too high, ATES investments are deemed too risky.

Maximum head change is strongly linked to aquifer horizontal hydraulic conductivity (Fig. 5, Fig. 11), as predicted by Darcy's law: higher conductivity reduces head changes (Fig. 13a). Conversely, there is no clear relation when comparing maximum head change to either total aquifer thickness or flow rate (Fig. 13b, 13c). It makes detailed knowledge of hydraulic conductivity more critical during early feasibility studies. This said, there is still considerable spreading or uncertainty around the trend in Fig. 13a. It reflects the influence of other sensitive variables, such as flow rate and total aquifer thickness, and minor contributions from less sensitive parameters. Ultimately, the exact head change depends on the combined effect of all hydrogeological properties (Fig. 11).

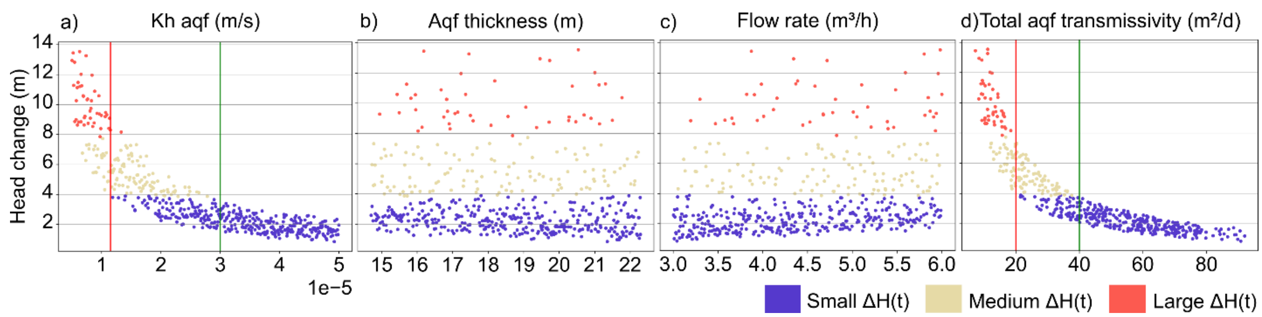

Fig. 13 Comparison of the head change with different sensitive parameters. The criteria for decision-making are indicated in red and green

As such, knowledge of total aquifer thickness further reduces prediction uncertainty. In Figure 13d, we compare total transmissivity of aquifer layers with the maximum head change, combining two key subsurface properties. To enhance the generalizability of the results, the criteria for hydraulic feasibility, previously defined based on hydraulic conductivity, can be expressed in terms of transmissivity. Conditions where total aquifer transmissivity is below 20 m^2/d should be avoided, whereas for a transmissivity exceeding 40 m^2/d hydraulic feasibility is guaranteed. In this relationship, (maximum design) flow rate remains a source of uncertainty on the prediction, despite being an engineering action controlled by the ATES user.

To determine the likelihood of certain head changes occurring, head change, total transmissivity and flow rate are evaluated together in a 3D parameter space with KDE. For a given flow rate, a 2D slice of the KDE is made to model the relation between transmissivity and head changes. Subsequently, for a given (estimated) transmissivity, a 1D slice of the KDE gives the likelihood of exceeding a certain head change, constrained by knowledge of the flow rate. Fig 14 illustrates this, for the same transmissivity, a higher flow rate will result in larger head changes. While there was no direct relationship between flow rate and maximum head change in Figure 13c, knowledge of the flow rate significantly refines the prediction. When the constrained density function is normalized, the probability of excessive injection pressure can be calculated and communicated to the investor. For example, suppose that the maximum allowable head change in a setting with total aquifer transmissivity of 21 m^2/d is 7.5 m. At a flow rate of 5.4 m^3/h Figure 15 shows that the probability of head changes below 7.5 m is 51 %. The probability increases to 88 % when limiting the flow rate to 3.4 m^3/h. In summary, this illustrates that uncertainty quantification, proposed in the workflow (Fig.

2), can determine the risk of an investment. Moreover, since subsurface properties are fixed, it can inform the investor about the impact of engineering actions to mitigate the risk.

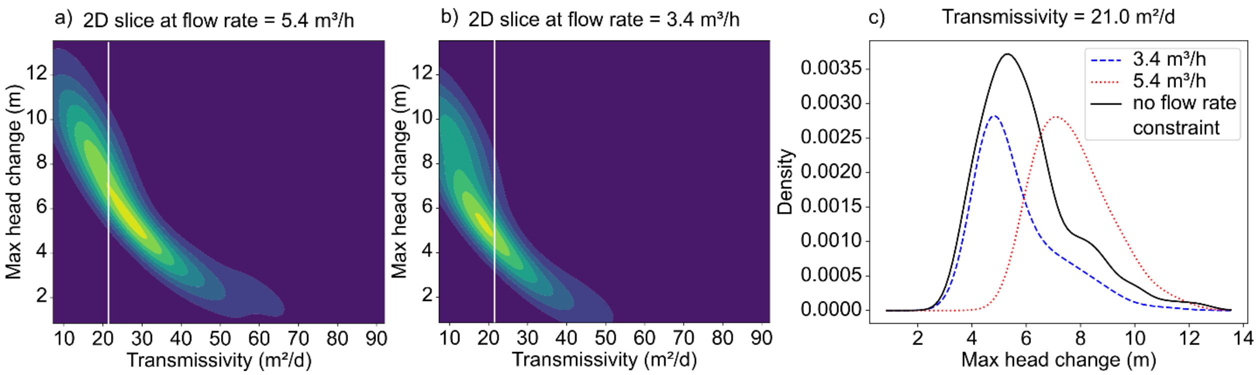

Fig. 14 Results of a 3D kernel density estimation. Two 2D slices were made: one for a high (a) and one for a low flow rate (b). A 1D slice for a transmissivity of 21 m^2/d subsequently illustrates the likelihood of head changes occurring, constrained by the knowledge of the flow rate (c). The density distribution shown in c is not normalized

5. Discussion

5.1. Reducing prediction uncertainty with field data

During a feasibility study for ATES, field data can be highly informative to reduce prediction uncertainty. Field campaigns must be designed to provide information related to crucial subsurface properties, which depend on the hydrogeological settings for storage and the prediction target. Sensitivity analyses provide valuable insights into selecting field data to narrow down model uncertainties. The field tests must be sensitive to the same parameters as the prediction, otherwise, the test will not effectively reduce uncertainty on parameters that matter for the prediction. Hydraulic conductivity, longitudinal dispersion, and — for small well spacings — layer thickness and porosity are the main subsurface properties influencing the prediction of hydraulic and thermal efficiency of ATES in low-transmissivity settings.

For low-transmissivity aquifers, limiting the maximum head change is critical. Therefore pumping and injection tests will provide informative field data to reduce uncertainty on the hydraulic feasibility. They give direct information on the head change, as well as estimate transmissivity (Lebbe et al., 1992). Accurately determining aquifer layer thickness with electromagnetic measurements, cone penetration tests or gamma ray logging also improves the prediction. When aiming for a small inter-well distance, simultaneous pumping and injection tests exploring hydraulic interactions are recommended (Tas et al., 2023).

Field tests sensitive to $\Delta T(t)$ are particularly important for these small inter-well distances, as thermal breakthroughs are detrimental to the efficiency. Heat tracer or push-pull tests mimic ATES behavior with a single well and offer information on thermal, and potentially hydraulic, feasibility (Vandenbohede et al., 2008; Wildemeersch et al., 2014; Hermans et al., 2019; De Schepper et al., 2020).

The proposed field strategy that was derived from the sensitivity analyses differs for other hydrogeological settings (Tas et al., 2025). Sensitivity analyses of ATES in sandy productive aquifers and shallow alluvial aquifers show that horizontal hydraulic conductivity and natural hydraulic gradient matter most for the prediction of thermal recovery efficiency. Hydraulic pressure constraints are absent, and thermal losses from natural groundwater flow dominate. Therefore, in traditional ATES settings and in settings with high natural groundwater flow velocity, Darcy flux measurements, combining both sensitive parameters, are most effective at reducing uncertainty on efficiency.

To carry out the proposed field tests, it will often be required to drill a new well if no existing wells are available with screens adapted to target maximum aquifer capacity. This introduces a new element to the decision-making process which is deciding about an intermediate investment (of a few 1000 euros) to reduce uncertainty and reach the decision. Field tests are highly effective in reducing uncertainty but they come with a high cost and often only provide local information (Hermans et al., 2023). When there are no immediate funds to gather field data, the strength of the proposed workflow and decision tree is that it can still provide risk assessment support based on literature information. To account for questionable accuracy or limited representativeness of literature estimates, the proposed UQ method based on joint probability distribution estimation can make use of the probability distribution for the parameters to assess the risk. Alternatively, when field data is available, it can be used for a more advanced UQ approach which includes uncertainty on sensitive parameters. For instance, the Bayesian Evidential Learning method aims to make long-term predictions from short-term field tests (Hermans et al., 2018; Athens and Caers, 2019). It relies on finding a direct relationship between data and prediction with statistical modelling.

5.2. Validity of the results

5.2.1. Applicability

The approach of building a decision tree is valid for any hydrogeological setting for storage. The quantitative results of this study are valid only for ATES systems within the considered ranges of the prior distributions (Table 1) and for settings with similar maximum allowable head change. Different settings require separate analyses to conclude on the most informative field strategy and criteria to decide upon the investment (Tas et al., 2025).

In this study, criteria on hydraulic conductivity and transmissivity for the decision tree are established. The derived criteria for which feasibility/infeasibility is guaranteed are close to each other. In practice, they might often be too similar when considering the accuracy of an initial estimate from literature. This highlights the importance of the uncertainty quantification based on joint probability distribution estimation that is proposed in the method, as one will quickly have to resort to it. The presented criteria are also based on a well spacing of 40 m. Sensitivity analyses for the 60 m and 80 m scenarios revealed fewer sensitive and critical parameters, yet the key factors influencing predictions remained consistent. This corroborates that the findings also apply to larger well spacings. In fact, the probability density function for uncertainty quantification of the maximum head change (Fig. 14) becomes slightly narrower, as fewer sensitive parameters significantly contribute to the overall variability. A consistent shift of the density distribution towards larger head changes is observed. This confirms that larger distances between the wells are less optimal for hydraulic feasibility. For well spacings smaller than those considered in this study, it is advised to carefully evaluate the risk of thermal breakthroughs with additional modelling or field tests.

This study's uncertainty quantification focused on predicting the maximum head change. The prediction in section 4.3 was constrained by knowledge of the flow rate and a transmissivity estimate. In practice, when resources allow for pumping-injection tests, the maximum head change can be directly observed and uncertainty quantification of transmissivity is more useful. To do this, the same 3D KDE relation can be used. The derived transmissivity prediction, along with knowledge of its likelihood to account for uncertainty, can be used in a detailed modelling study of the full ATES system.

5.2.2. Model simplifications

The models aim to represent realistic scenarios, however, certain simplifications have been made. First, only a single well pair is simulated, whereas in reality, multiple pairs would be required to meet energy demand. When ATES is deemed feasible in a low transmissivity setting, the full system must be modelled in detail. This aims to optimize well placement for hydraulic and thermal efficiency, as well as optimal subsurface space usage (Bloemendal et al., 2018; Tas et al., 2023). Second, the simulation period is limited to the first three years of operation, even though a dynamic equilibrium of $\Delta T(t)$ is typically reached only after 5+ years. Therefore, the efficiencies in Figure 8 may still increase in subsequent storage and recovery cycles. This simplification limits the computational demand and does not affect the clustering or sensitivity analysis. The efficiency calculation is also less crucial for feasibility, it is sufficient to avoid thermal breakthrough conditions. Finally, the modeled system assumes an energetically balanced operation, meaning that both storage seasons have equal durations and flow rates. In practice, an unbalanced system cannot be excluded. Only in the Netherlands are regulations on heating-cooling balance in place (Heimovaara and Trcka, 2012; Lieten et al., 2012). An unbalanced system does not compromise hydraulic feasibility because it is not allowed to exceed the design flow rate. The thermal recovery efficiency, however, can significantly reduce when the warm and cold stored volumes are not equal. Over time, stored thermal energy may be depleted, leading to the extraction of water at its natural temperature. Furthermore, if the stored volume exceeds predictions, the risk for thermal breakthrough increases.

5.2.3. Numerical challenges

Figure 7 shows $\Delta T(t)$ for all three scenarios. These results are influenced by numerical dispersion, illustrated by the unexplained peaks at the beginning of the simulation period. At the start of each season, it manifests as a sudden drop in ΔT. This numerical effect is more pronounced for smaller well spacings but diminishes with each successive storage cycle. The same solver settings for heat transport were applied for all three scenarios. While these settings were appropriate for the 80 m scenario, the maximum transport step size should have been reduced for the 60 m and 40 m scenarios. In these cases, where well interactions are more complex, a stricter stability criterion is required. The numerical dispersion only affects thermal simulations. It does not impact clustering as all model realizations are affected in the same way. Additionally, comparison with a model with more stringent settings confirmed that the numerical dispersion does not affect the course of the rest of the curve. Therefore, the results remain valid and we did not rerun all models. This highlights that no single set of solver settings is suitable for each model realization, which is a fundamental challenge of applying stochastic simulations for hydrogeological applications. It also shows that running very detailed and complex simulations has limited value for stochastic analyses of ATES systems: it significantly increases runtimes yet does not affect the outcome (Knowling et al., 2019).

6. Conclusion (decision tree)

This paper develops a novel workflow to draw a decision tree that supports go/no go investment decisions for aquifer thermal energy storage systems in complex hydrogeological settings. It allows for the exploration of a project's feasibility before investing in field tests. Its potential is illustrated by applying it to a low-transmissivity setting: a currently challenging target for ATES because the system should operate close to maximum aquifer capacity, which itself is uncertain. The workflow consecutively consists of the definition of the prediction targets and prior distribution, Monte Carlo simulations, distance-based global sensitivity analysis and uncertainty quantification through joint probability distribution estimation. It allows to better understand storage conditions and the role of engineering actions in mitigating the risk. In the analyzed low-transmissivity setting, aquifer hydraulic conductivity, thickness and flow rate dominate hydraulic feasibility, while longitudinal dispersion, flow rate and well spacing significantly impact thermal efficiency. The decision tree combines all insights of this stochastic analysis and provides a graphical guideline for improved feasibility studies (Figure 15). In essence, it consists of connections between the prediction targets, the most informative subsurface properties, intermediate decisions or actions that can reduce the investment risk, and the final decision. Figure 15 suggests the following approach:

1) Estimate horizontal hydraulic conductivity and/or total transmissivity of aquifer layers.
    a. When horizontal hydraulic conductivity or transmissivity exceeds (Fig. 13d) some feasibility criteria (feas_crit), the maximum head change will be acceptable. These criteria correspond to 3E-5 m/s and 40 m^2/d respectively for the case study. Thermal recovery efficiency should be evaluated separately.
    b. When conductivity or transmissivity is below the critical criteria (infeas_crit) (Fig. 13d), the case should be abandoned because head changes will be excessive. These criteria correspond to 1.15E-5 m/s and 20 m^2/d respectively for the case study.
    c. When an initial literature estimate indicates values between these limits or when they lack sufficient precision, uncertainty quantification is required for risk assessment.
2) Next, we predict thermal energy efficiency which is essential when working with smaller inter-well distances.
    a. When minimum efficiency requirements are lacking, it is sufficient to rule out conditions that lead to a thermal breakthrough. The risk might be nonexistent depending on the distance between wells. If the risk exists, combinations of parameters leading to this situation can be identified and appropriate field tests can be proposed such as hydraulic tests, thermal tracer tests or push-pull tests.
    b. When a minimum efficiency is required, the UQ method proposed for the prediction of $\Delta H(t)$ can be applied to $\Delta T(t)$.
3) For edge cases (1c, 2a, 2b), we should adapt engineering actions to limit the financial risk. For instance, increasing the injection temperature difference allows us to decrease the flow rate per well. This mitigates the risk of excessive injection pressures and thermal breakthroughs. Alternatively, we can increase the inter-well distance to improve thermal recovery efficiency.
4) When ATES is deemed feasible in the low-transmissivity setting, detailed modeling of the full system should be performed to optimize well placement. Insensitive parameters can be simplified to average values. Hydraulic feasibility is critical and optimal energy efficiency (and density) is desirable.

In summary, with the proposed workflow and decision tree approach, this study aims to optimize feasibility studies, improve the cost-efficiency of planned field studies, and move new ATES project developments forward.

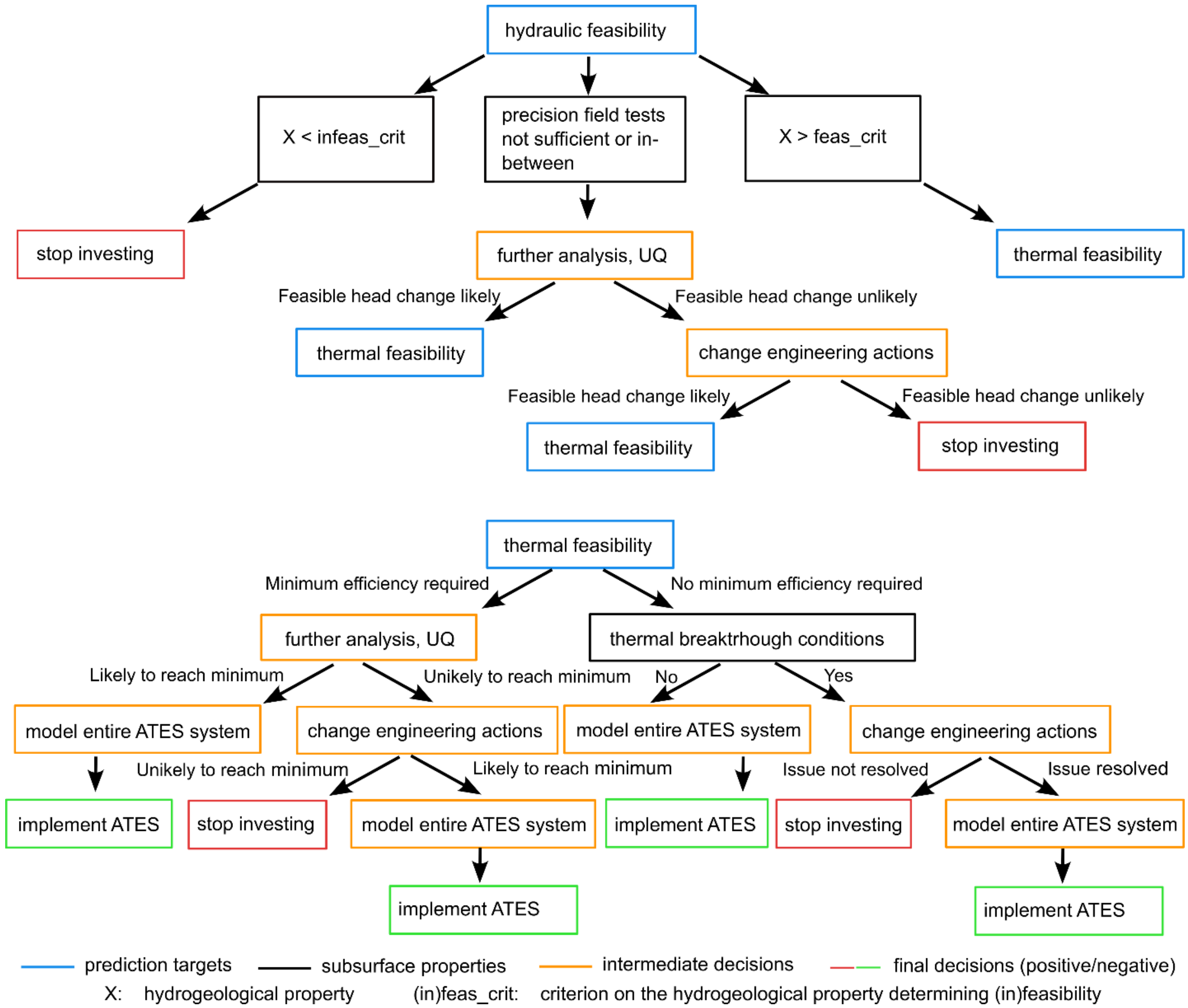

Fig. 15 Decision tree for ATES in hydrogeological settings where hydraulic feasibility is crucial (primary root node) and thermal feasibility desirable (secondary root node)

7. Data availability statement

The input and output data of the simulations generated and used for the DGSA's of this study are openly available on Zenodo https://doi.org/10.5281/zenodo.15119419. The scripts used to process the input and output are available on GitHub https://github.com/lukatas/ATES_SensitivityAnalyses.

8. Acknowledgements

We would like to express our sincere thanks to the DIAMONDS project team and stakeholders for the fruitful discussions and for offering new perspectives on the sustainable use of the subsurface. Finally, we truly appreciate the support of Ghent University policymakers in establishing a living lab

on campus (low-transmissivity setting) [(info sustainability research living lab UGent)] This allows us to continue to explore the potential of ATES in environments beyond the current state of the art.

9. Competing Interests

The authors have no relevant financial or non-financial interests to disclose

10. Author Contributions

All authors contributed to the study conception and design. Validation, formal analysis and funding acquisition were performed by Thomas Hermans and Luka Tas. Material preparation, data collection & curation, software and visualization were performed by Luka Tas. Thomas Hermans was the formal supervisor. The first draft of the manuscript was written by Luka Tas and all authors commented on previous versions of the manuscript. All authors read and approved the final manuscript.

11. Funding

Luka Tas has received funding from FWO (grant number: 1SH0M24N). The resources and services used in this work were provided by the VSC (Flemish Supercomputer Center), funded by the Research Foundation - Flanders (FWO) and the Flemish Government and the strategic basic research project DIAMONDS (grant number S001324N).

References

Athens, N.D., Caers, J.K., 2019. A Monte Carlo-based framework for assessing the value of information and development risk in geothermal exploration. Applied Energy 256, 113932. https://doi.org/10.1016/j.apenergy.2019.113932

Bakker, M., Post, V., Langevin, C.D., Hughes, J.D., White, J.T., Starn, J.J., Fienen, M.N., 2016. Scripting MODFLOW Model Development Using Python and FloPy. Groundwater 54, 733–739. https://doi.org/10.1111/gwat.12413

Bedekar, V., Morway, E.D., Langevin, C.D., Tonkin, M.J., 2016. MT3D-USGS: Groundwater Solute Transport Simulator for MODFLOW. https://doi.org/10.5066/F75T3HKD

Beernink, S., Barnhoorn, A., Vardon, P., Bloemendal, M., Hartog, N., 2022. Impact of vertical layering and the uncertainty and anisotropy of hydraulic conductivity on HT-ATES performance.

Bloemendal, M., Hartog, N., 2018. Analysis of the impact of storage conditions on the thermal recovery efficiency of low-temperature ATES systems. Geothermics 71, 306–319. https://doi.org/10.1016/j.geothermics.2017.10.009

Bloemendal, M., Jaxa-Rozen, M., Olsthoorn, T., 2018. Methods for planning of ATES systems. Applied Energy 216, 534–557. https://doi.org/10.1016/j.apenergy.2018.02.068

Databank Ondergrond Vlaanderen, (Database Underground Flanders), n.d. Verkenner (Explorer).

Davies, D.L., Bouldin, D.W., 1979. A Cluster Separation Measure. IEEE Trans. Pattern Anal. Mach. Intell. PAMI-1, 224–227. https://doi.org/10.1109/TPAMI.1979.4766909

De Paoli, C., Duren, T., Petitclerc, E., Agniel, M., Dassargues, A., 2023. Modelling Interactions between Three Aquifer Thermal Energy Storage (ATES) Systems in Brussels (Belgium). Applied Sciences 13, 2934. https://doi.org/10.3390/app13052934

De Schepper, G., Bolly, P.-Y., Vizzotto, P., Wecxsteen, H., Robert, T., 2020. Investigations into the First Operational Aquifer Thermal Energy Storage System in Wallonia (Belgium): What Can Potentially Be Expected? Geosciences 10, 33. https://doi.org/10.3390/geosciences10010033

Doughty, C., Hellström, G., Tsang, C.F., Claesson, J., 1982. A dimensionless parameter approach to the thermal behavior of an aquifer thermal energy storage system. Water Resources Research 18, 571–587. https://doi.org/10.1029/WR018i003p00571

Duijff, R., Bloemendal, M., Bakker, M., 2021. Interaction Effects Between Aquifer Thermal Energy Storage Systems. Groundwater 61, 173–182. https://doi.org/10.1111/gwat.13163

European Commission, 2016. An EU Strategy on Heating and Cooling. Communication from the Commission to the European Parliament, The Council, the European Economic and Social Committee and the Committee of the Regions; European Commission: Brussels, Belgian, 2016.

Fenwick, D., Scheidt, C., Caers, J., 2014. Quantifying Asymmetric Parameter Interactions in Sensitivity Analysis: Application to Reservoir Modeling. Math Geosci 46, 493–511. https://doi.org/10.1007/s11004-014-9530-5

Ferré, T.P.A., 2017. Revisiting the Relationship Between Data, Models, and Decision-Making. Groundwater 55, 604–614. https://doi.org/10.1111/gwat.12574

Fleuchaus, P., Godschalk, B., Stober, I., Blum, P., 2018. Worldwide application of aquifer thermal energy storage – A review. Renewable and Sustainable Energy Reviews 94, 861–876. https://doi.org/10.1016/j.rser.2018.06.057

François, L., Van Lysebetten, G., 2017. Code van goede praktijk. Ontwerp, uitvoering en beheer van koude-warmteopslagsystemen in de ondipe ondergrond in Vlaanderen. (WTCB).

Glassley, W.E., 2015. Geothermal Energy: Renewable Energy and the Environment, Second Edition, 2nd ed. CRC Press, Boca Raton. https://doi.org/10.1201/b17521

Harbaugh, A.W., Langevin, C.D., Hughes, J.D., Niswonger, R.G., Konikow, L.F., 2017. MODFLOW-2005: USGS three-dimensional finite-difference groundwater model. https://doi.org/10.5066/F7RF5S7G

Hecht-Méndez, J., Molina-Giraldo, N., Blum, P., Bayer, P., 2010. Evaluating MT3DMS for Heat Transport Simulation of Closed Geothermal Systems. Groundwater 48, 741–756. https://doi.org/10.1111/j.1745-6584.2010.00678.x

Heimovaara, T.J., Trcka, M., 2012. Onderzoek criteria energiebalans WKO. DWA installatie- en energieadvies & IF Technology.

Heldt, S., Beyer, C., Bauer, S., 2024. Uncertainty assessment of thermal recovery and subsurface temperature changes induced by high-temperature aquifer thermal energy storage (HT-ATES): A case study. Geothermics 122, 103086. https://doi.org/10.1016/j.geothermics.2024.103086

Hermans, T., Goderniaux, P., Jougnot, D., Fleckenstein, J.H., Brunner, P., Nguyen, F., Linde, N., Huisman, J.A., Bour, O., Lopez Alvis, J., Hoffmann, R., Palacios, A., Cooke, A.-K., Pardo-Álvarez, Á., Blazevic, L., Pouladi, B., Haruzi, P., Fernandez Visentini, A., Nogueira, G.E.H., Tirado-Conde, J., Looms, M.C., Kenshilikova, M., Davy, P., Le Borgne, T., 2023. Advancing measurements and representations of subsurface heterogeneity and dynamic processes: towards 4D hydrogeology. Hydrology and Earth System Sciences 27, 255–287. https://doi.org/10.5194/hess-27-255-2023

Hermans, T., Lesparre, N., De Schepper, G., Robert, T., 2019. Bayesian evidential learning: a field validation using push-pull tests. Hydrogeol J 27, 1661–1672. https://doi.org/10.1007/s10040-019-01962-9

Hermans, T., Nguyen, F., Klepikova, M., Dassargues, A., Caers, J., 2018. Uncertainty Quantification of Medium-Term Heat Storage From Short-Term Geophysical Experiments Using Bayesian Evidential Learning. Water Resources Research 54, 2931–2948. https://doi.org/10.1002/2017WR022135

Hopmans, J.W., Šimunek, J., Bristow, K.L., 2002. Indirect estimation of soil thermal properties and water flux using heat pulse probe measurements: Geometry and dispersion effects. Water Resources Research 38, 7-1-7–14. https://doi.org/10.1029/2000WR000071

Hughes, J.D., Langevin, C.D., Paulinski, S.R., Larsen, J.D., Brakenhoff, D., 2024. FloPy Workflows for Creating Structured and Unstructured MODFLOW Models. Groundwater 62, 124–139. https://doi.org/10.1111/gwat.13327

Jackson, M.D., Regnier, G., Staffell, I., 2024. Aquifer Thermal Energy Storage for low carbon heating and cooling in the United Kingdom: Current status and future prospects. Applied Energy 376, 124096. https://doi.org/10.1016/j.apenergy.2024.124096

Kaufman, L., Rousseuw, P.J., 1990. Review of Finding Groups in Data: An Introduction to Cluster Analysis. https://doi.org/10.2307/2532178

Knowling, M.J., White, J.T., Moore, C.R., 2019. Role of model parameterization in risk-based decision support: An empirical exploration. Advances in Water Resources 128, 59–73. https://doi.org/10.1016/j.advwatres.2019.04.010

Konikow, L.F., Hornberger, G.Z., Halford, K.J., Hanson, R.T., Harbaugh, A.W., 2009. Revised multi-node well (MNW2) package for MODFLOW ground-water flow model (No. 6-A30), Techniques and Methods. U.S. Geological Survey. https://doi.org/10.3133/tm6A30

Lebbe, L., Mahauden, M., De Breuck, W., 1992. Execution Of A Triple Pumping Test And Interpretation By An Inverse Numerical Model. HYJO 1, 20–34. https://doi.org/10.1007/PL00010967

Lieten, S., de Vries, E., van Baaren, E., Bakr, M., Oude Essink, G., Hartog, N., Meinderstma, W., van Nieuwkerk, E., van Oostrom, N., Woning, M., Drijver, B., Krajenbrink, H., Mathijssen, H., Wennekes, R., 2012. Literatuuronderzoek Meer met Bodemenergie.

Lu, D., Ricciuto, D., 2020. Efficient Distance-based Global Sensitivity Analysis for Terrestrial Ecosystem Modeling, in: 2020 International Conference on Data Mining Workshops (ICDMW). Presented at the 2020 International Conference on Data Mining Workshops (ICDMW), IEEE, Sorrento, Italy, pp. 324–332. https://doi.org/10.1109/ICDMW51313.2020.00052

NVOE, 2021. Werkwijzen en richtlijnen ondergrondse energieopslag.pdf.

Park, J., Yang, G., Satija, A., Scheidt, C., Caers, J., 2016. DGSA: A Matlab toolbox for distance-based generalized sensitivity analysis of geoscientific computer experiments. Computers & Geosciences 97, 15–29. https://doi.org/10.1016/j.cageo.2016.08.021

Ramos-Escudero, A., García-Cascales, M.S., Urchueguía, J.F., 2021. Evaluation of the Shallow Geothermal Potential for Heating and Cooling and Its Integration in the Socioeconomic Environment: A Case Study in the Region of Murcia, Spain. Energies 14, 5740. https://doi.org/10.3390/en14185740

Regnier, G., Firth, H.T., Jackson, M.D., 2023. Aquifer Thermal Energy Storage in the UK: current status and challenges to uptake (No. EGU23-11492). Presented at the EGU23, Copernicus Meetings. https://doi.org/10.5194/egusphere-egu23-11492

Renard, P., 2007. Stochastic Hydrogeology: What Professionals Really Need? Groundwater 45, 531–541. https://doi.org/10.1111/j.1745-6584.2007.00340.x

Scheidt, C., Li, L., Caers, J., 2018. Quantifying Uncertainty in Subsurface Systems, 1st ed, Geophysical Monograph Series. Wiley. https://doi.org/10.1002/9781119325888

Silverman, B.W., 1986. Density estimation for statistics and data analysis. 37(1), 1–22. Monographs on Statistics and Applied Probability 37, 1–22.

Silvestri, V., Crosta, G., Previati, A., Frattini, P., Bloemendal, M., 2025. Uni-directional ATES in high groundwater flow aquifers. Geothermics 125, 103152. https://doi.org/10.1016/j.geothermics.2024.103152

Sommer, W., Valstar, J., Leusbrock, I., Grotenhuis, T., Rijnaarts, H., 2015. Optimization and spatial pattern of large-scale aquifer thermal energy storage. Applied Energy 137, 322–337. https://doi.org/10.1016/j.apenergy.2014.10.019

Sommer, W., Valstar, J., van Gaans, P., Grotenhuis, T., Rijnaarts, H., 2013. The impact of aquifer heterogeneity on the performance of aquifer thermal energy storage. Water Resources Research 49, 8128–8138. https://doi.org/10.1002/2013WR013677

Stemmle, R., Hanna, R., Menberg, K., Østergaard, P.A., Jackson, M., Staffell, I., Blum, P., 2024. Policies for aquifer thermal energy storage: international comparison, barriers and recommendations. Clean Techn Environ Policy. https://doi.org/10.1007/s10098-024-02892-1

Tas, L., Hartog, N., Bloemendal, M., Simpson, D., Robert, T., Thibaut, R., Zhang, L., Hermans, T., 2025. Efficiency and heat transport processes of low-temperature aquifer thermal energy storage systems: new insights from global sensitivity analyses. Geothermal Energy 13, 2. https://doi.org/10.1186/s40517-024-00326-1

Tas, L., Simpson, D., Hermans, T., 2023. Assessing the potential of low-transmissivity aquifers for aquifer thermal energy storage systems: a case study in Flanders (Belgium). Hydrogeol J 31, 2363–2380. https://doi.org/10.1007/s10040-023-02696-5

Vandenbohede, A., Hermans, T., Nguyen, F., Lebbe, L., 2011. Shallow heat injection and storage experiment: Heat transport simulation and sensitivity analysis. Journal of Hydrology 409, 262–272. https://doi.org/10.1016/j.jhydrol.2011.08.024

Vandenbohede, A., Louwyck, A., Lebbe, L., 2008. Heat transport in a push-pull test: parameter identification and sensitivity analyses, in: IAHS Publication. Presented at the 6th International conference on Calibration and Reliability in Groundwater Modelling (ModelCARE 2007) : Credibility of modelling, International Association of Hydrological Sciences (IAHS), pp. 257–261.

Vandenbohede, A., Louwyck, A., Vlamynck, N., 2014. SEAWAT-Based Simulation of Axisymmetric Heat Transport. Groundwater 52, 908–915. https://doi.org/10.1111/gwat.12137

White, J.T., Doherty, J.E., Hughes, J.D., 2014. Quantifying the predictive consequences of model error with linear subspace analysis. Water Resources Research 50, 1152–1173. https://doi.org/10.1002/2013WR014767

White, J.T., Knowling, M.J., Moore, C.R., 2020. Consequences of Groundwater-Model Vertical Discretization in Risk-Based Decision-Making. Groundwater 58, 695–709. https://doi.org/10.1111/gwat.12957

Wildemeersch, S., Jamin, P., Orban, P., Hermans, T., Klepikova, M., Nguyen, F., Brouyère, S., Dassargues, A., 2014. Coupling heat and chemical tracer experiments for estimating heat transfer parameters in shallow alluvial aquifers. Journal of Contaminant Hydrology, Selected papers from The 8th International Association of Hydrological Sciences (IAHS) Groundwater Quality Conference 2013 (GQ13) - Managing groundwater quality to support competing human and ecological needs 169, 90–99. https://doi.org/10.1016/j.jconhyd.2014.08.001

Winter, C.L., 2004. Stochastic hydrology: practical alternatives exist. Stochastic Environmental Research and Risk Assessment 18, 271–273. https://doi.org/10.1007/s00477-004-0198-0

Xu, T., Valocchi, A.J., 2015. A Bayesian approach to improved calibration and prediction of groundwater models with structural error. Water Resources Research 51, 9290–9311. https://doi.org/10.1002/2015WR017912

Zeghici, R.M., Oude Essink, G.H.P., Hartog, N., Sommer, W., 2015. Integrated assessment of variable density–viscosity groundwater flow for a high temperature mono-well aquifer thermal energy storage (HT-ATES) system in a geothermal reservoir. Geothermics 55, 58–68. https://doi.org/10.1016/j.geothermics.2014.12.006

Zhang, L., Dieudonné, A.-C., Daniilidis, A., Dong, L., Cao, W., Thibaut, R., Tas, L., Hermans, T., 2025. Thermo-hydro-mechanical modeling of geothermal energy systems in deep mines: Uncertainty quantification and design optimization. Applied Energy 377, 124531. https://doi.org/10.1016/j.apenergy.2024.124531

Zheng, C., 2010. MT3DMS v5.3 Supplemental User's Guide.

Zuurbier, K.G., Hartog, N., Valstar, J., Post, V.E.A., van Breukelen, B.M., 2013. The impact of low-temperature seasonal aquifer thermal energy storage (SATES) systems on chlorinated solvent contaminated groundwater: Modeling of spreading and degradation. Journal of Contaminant Hydrology 147, 1–13. https://doi.org/10.1016/j.jconhyd.2013.01.002